Low-Frequency Earthquakes along the Ryukyu Islands Triggered by Teleseismic Earthquakes

Ayumi Kinjo
University of the Ryukyus: Ryukyu Daigaku
Mamoru Nakamura (mnaka@sci.u-ryukyu.ac.jp)
University of the Ryukyus https://orcid.org/0000-0001-7627-0056

Express Letter

Keywords: Low-frequency earthquake, surface wave, slow earthquake, Ryukyu Trench

Posted Date: March 15th, 2021

DOI: https://doi.org/10.21203/rs.3.rs-284600/v1

Abstract

Tremors and low-frequency earthquakes (LFEs), which occur in the plate interface, can provide useful information about the state of aseismic stress transfer in mega-earthquake fault zones. We estimated the distribution of stress sensitivity in the subducted plate interface by using triggered LFEs. Specifically, we detected LFEs in the Ryukyu Trench triggered by the surface waves of large teleseismic earthquakes by using the waveform records of broadband and short-period seismometers installed in the Ryukyu Arc. We selected a total of 45 teleseismic earthquakes with magnitudes of more than 7.5, which occurred between 2004 and 2017, for the analysis. We could detect the triggered LFEs for five teleseismic earthquakes. Then, we determined the hypocenters of LFEs by using the relative arrival times of LFEs for each station. The LFEs were distributed in the south of Okinawa Island and the Yaeyama area. Moreover, they were distributed around the source fault of the slow slip events. These were almost the same as the position of LFEs accompanying very low-frequency earthquakes (VLFEs). However, the epicenters of the triggered LFEs were concentrated near the locations of the most active LFE clusters accompanying VLFEs. This suggests that the sensitivity for inducing LFEs was higher near the most active clusters of the LFEs accompanying the VLFEs. The amplitudes of the triggered LFEs were proportional to the peak ground velocity of the surface waves. This indicates that the LFEs accompanying VLFEs are activated by stress acceleration in the Yaeyama and Okinawa areas and the triggered LFEs observed in these areas can be a result of the activation of the ambient tremors due to increased stress.

1. Introduction

The activity of non-volcanic tremors, which are one type of slow earthquake, in the plate interface can provide useful information about the movement of aseismic slip in mega-thrust fault zones, and such data can be indicative of the heterogeneity of stress sensitivity and aseismic stress accumulation in the plate interface (Obara and Kato 2016). These tremors have characteristics similar to regular earthquakes such as a long-duration, emergent onset, and lack of high-frequency components of wave energy. The tremors have been observed in various areas around the circum-Pacific plate boundaries (Obara 2002; Rogers and Dragert 2003; Nadeau and Dolenc 2005; Payero et al. 2008; Fry et al. 2011; Obara and Kato 2016). Before 2009, tremors that occurred in the down-dip extension of the seismogenic zone had been observed, but later, those that occurred in the up-dip extension were detected (Obara and Kodaira 2009; Walter et al. 2011; Ito et al. 2015; Yamashita et al. 2015; Tanaka et al. 2019). The existence of these tremors and activity changes induced by external stress implies that aseismic slip proceeds in the up-dip and down-dip of the plate interface, and the stress sensitivity in the up-dip and down-dip of the plate interface is extremely weak in these areas.

We focused on triggered tremors (i.e., low-frequency earthquakes or LFEs) caused by dynamic stress changes to estimate the distribution of stress sensitivity in the plate interface within the Ryukyu subduction zone. Although tremors usually have occurred as ambient tremors, those triggered by the surface waves of teleseismic earthquakes also have been observed (Miyazawa and Mori 2006; Rubinstein et al. 2007; Peng et al. 2008; Gomberg et al. 2008; Chao et al. 2012b; Chao et al. 2013). The

characteristics of the triggered tremors are similar to those of the ambient tremors, and so is their mechanism. Therefore, the detection of triggered tremors can implicate the existence of ambient tremors (Gomberg 2010; Fry et al. 2011; Ide 2012; Chao et al. 2013; Sun et al. 2015).

Tremors triggered by the surface waves of large earthquakes also have been observed in the Ryukyu Trench. Chao and Obara (2016) reported that a tremor (LFE) was detected in the high-frequency component of a broadband seismometer when the surface waves of a M8-class teleseismic earthquake passed over the Yaeyama area, to the southwest of the Ryukyu Trench. Because the tremors were observed at stations IGK and YNG of the F-net, which were established by the National Research Institute for Earth Science and Disaster Resilience (NIED) (Fig. 1), in the Yaeyama area, tremors were also assumed to have occurred in the Ryukyu Trench. However, because the Fnet observation network has only two stations (IGK and YNG) in the Yaeyama area, it is a difficult task to determine the detailed hypocenter distribution of the tremors.

In this study, we detected the triggered LFEs, determined their hypocenters, and estimated the distribution of stress sensitivity in the Ryukyu subduction zone. We used the waveforms of the short-period seismic network operated by the Japan Meteorological Agency (JMA). This observation network of the short-period seismographs with a natural period of 1 s is distributed in the Ryukyu Islands. Because these seismographs are installed on the ground, the noise level of the waveforms is higher than that of borehole-type seismographs. Although these seismographs are not suitable for detecting weak signals, LFEs can be detected by this seismic network in some cases. Nakamura (2017) detected and located VLFE-LFEs from the waveforms of the JMA's short-period seismic network. The LFEs were clustered to the south of the Hateruma and Ishigaki islands, the area south of Okinawa Island, and the area northeast of Okinawa Island. If the LFEs occurred on the plate interface, their depths corresponded to 15–20 km. According to the OBS survey conducted in the south of the Yaeyama area, the LFEs occurred on the subducting plate interface (Arai et al. 2016). The difference of distribution of the ambient and triggered LFEs can inform us about the lateral heterogeneity of stress sensitivity in the subducted plate interface.

2. Data And Methods

2.1 Data

Earthquakes that occurred between January 2004 and December 2017 with magnitudes of more than 7.5, epicentral distances ranging from 15 to 90 degrees from Okinawa Island, and depths shallower than 300 km were used in the analysis (a total of 45 events) (Fig. 1, Table S1). Broadband waveforms at IGK and ZMM of the Fnet observation network were used. The instrumental responses of the waveforms were corrected. The short-period seismic waveforms of the JMA, 3 h from the occurrence of the earthquake, were also used to detect the LFEs.

2.2 Detection of LFEs

The waveforms of the broadband seismometers were 0.02–0.05 Hz band-pass filtered to display the surface waves. The horizontal component waveforms of the short-period seismometer and Fnet seismometers were 2–4 Hz band-pass filtered to detect the LFEs. Potential wave groups of the LFEs when the surface waves passed were visually selected from the short-period seismograms (Fig. 2).

2.3 Hypocenter determination of LFEs

To determine the hypocenters of the LFEs, the arrival time difference of the wave group of the LFEs among the stations was calculated by using the envelope correlation method (Obara 2002). We first applied a band-pass filter of 2–4 Hz to the short-period and broadband seismograms, and then, we calculated the RMS amplitudes with a time-window of 10 s. We calculated the cross-correlations of the RMS waveforms between the two stations and picked the timing of the maximum cross-correlation, which is the arrival time difference between the two stations.

Next, we determined the hypocenters by using the grid-search method (Chao et al. 2013), which uses the arrival time difference among the stations. The arrival time difference when the cross-correlation was over 0.7 was used for the hypocenter determination. Since the waveforms of the LFEs were dominant with the S-wave, the S-wave velocity model was used in the grid-search method. The JMA2001 velocity model was used for the one-dimensional S-wave velocity structure (Ueno et al. 2002).

2.4 Comparison of the LFE amplitude with PGV

We compared the LFE amplitude with the PGV in the Okinawa and Yaeyama areas. We used a band-pass filter at 2–4 Hz for the waveforms at stations IGK and ZMM in the Yaeyama and Okinawa areas. Then, we computed the median amplitude of the filtered waveforms. For the waveforms of all events, the median amplitude 0–300 s prior to the occurrence of the earthquake was calculated as the background noise amplitude. The median amplitude of the filtered LFE waveforms was defined as the triggered LFE amplitude. We picked the PGV in the vertical and transverse components of the surface waves with no filter for all events. Next, we examined the relationship between PGV and the triggered LFE amplitude.

3. Results

3.1 Waveforms of the triggered LFEs

In the Yaeyama area, the LFEs were triggered during the passage of the surface wave of one teleseismic earthquake. Among 45 teleseismic earthquakes, LFEs were detected in five events in the Yaeyama area.

In the Sumatra earthquake (Mw 9.1) of December 26, 2004, the LFEs were observed in the Yaeyama area when the surface waves passed at 1300–1700 s (Fig. 2a). The LFEs first arrived at the HATERS station, and then, they were delayed at stations east and west of the HATERS station. The LFE activity started when the maximum amplitude of the Love wave arrived rather than that of the Rayleigh wave (Fig. 2a). In this earthquake, LFEs were observed even in the vicinity of Okinawa Island when the surface waves passed at 1500–1800 s (Fig. 3a). The LFEs arrived the earliest at ZMM or TAMAG2, and later at KUMEJ2

or KUNIGA stations. At 1500–1800 s, two predominant phases were observed at various stations. At TAMAG2 and ZMM, weak but possible LFEs were detected at 1600–1700 s. These phases were not observed at the other stations. The arrival time of these LFEs corresponded to those of the maximum amplitude of Love waves.

The LFEs were also observed in the waveforms of the Nias earthquake on March 28, 2005 (Mw8.6). However, the amplitudes of the LFE were the smallest among the five events in which LFEs were observed. The LFEs were observed at stations to the northeast of the HATERS station when the maximum amplitude of the Rayleigh wave arrived in the Yaeyama area (1100 s after the earthquake) (Fig. 2b). The LFEs were also observed in the Okinawa area during the passage of the surface waves (at approximately 1700 s) (Fig. 3b). The LFEs rapidly reached TAMAG2 and ZMM in the Okinawa area. The arrival time was closer to the passage time of the maximum amplitude of the Love wave (1600 s) than that of the Rayleigh wave (1200 s).

In the Wenchuan earthquake of 2008 (Mw7.9), LFEs were observed in the Yaeyama area when the surface waves passed at 700–900 s (Fig. 2c). The arrival of the LFEs was the fastest at the HATERS station. The LFEs were observed around the arrival of the maximum amplitude of the Love waves in the Yaeyama area. Similar LFEs were observed in Okinawa at 900–1000 s. The LFEs were first observed at ZMM and TAMAG2 at 950 s, which was the arrival time of the maximum amplitude of the Rayleigh wave in Okinawa.

In the Sumatra earthquake of 2012 (Mw8.6), LFEs were observed in the Yaeyama area at 1500–2000 s (Fig. 2d). The LFEs were first observed at the HATERS station and then at YONAGU. The LFEs intermittently continued after the passage of the maximum amplitude of the surface wave (Rayleigh waves and Love waves). Even in Okinawa, significant arrivals of LFEs were observed at 1300, 1600, and 1800 s (Fig. 3d). The LFEs were observed around the arrival time of the maximum peak of the surface wave.

In the Gorkha earthquake in Nepal on April 25, 2015 (Mw7.8), the LFEs were observed in the Yaeyama area when the surface wave passed at 1200–1400 s (Fig. 2e). In the waveform, the arrival of LFE at 1200 s corresponded to the maximum amplitude of the Love wave, and the arrival of LFE at 1400 s corresponded to the maximum amplitude of the Rayleigh wave. After the passage of the surface wave (1900 s or more), a plurality of LFEs were recorded at KUROSH, IGK, ISHIG2, and ISHIGH (Fig. 2e). The LFEs were observed around the maximum amplitude of the Love wave (1400–1600 s) even in the Okinawa area (Fig. 3e). The LFEs reached the TAMAG3 station the fastest. They were observed in the entire Okinawa area even after the surface wave passed at 1900 s. The LFEs were observed at ZMM, TAMAG2, KUNIGA, and NAGOT at 2150 s.

3.2 Hypocenter distribution

Seven LFEs were identified in the Yaeyama area (Fig. 4a, Table S2). The hypocenters of LFEs generated during the passage of the surface waves were distributed around 24.0°N and 123.6°E. The hypocenters of

LFEs, which occurred immediately after the passage of the surface waves, were scattered around 24.0°N and 123.6°E. The error in the determination of the hypocenter of LFEs in the 2004 event is shown by the contour lines in Fig. 4a. Since the depth determination was not accurate, the determination error at the depth of 0 km was plotted. The contour line extended in the N–S direction and had a large error in the direction perpendicular to the trench axis.

Seven LFEs were identified in the Okinawa area (Fig. 4b, Table S2). Most of the LFEs were distributed around 25.8°N and 127.7°E. The error of the hypocenter determination is shown by the contour lines in Fig. 4b. The contours extended obliquely to the trench axis, away from the seismic network near Okinawa Island. There was a large error in the direction away from the island. In the Okinawa area, the LFEs tended to occur separately, except for during the 2015 event. The hypocenters of the LFEs, which occurred immediately after the passage of the surface waves, were also distributed to the south of Okinawa Island. The difference in the distribution of the LFEs during and after the surface wave passage was not significant.

3.3 Relationship between PGV and the amplitude of LFEs

The triggered LFE amplitude during the passage of the surface wave showed a positive correlation with the PGV at ZMM and IGK for both vertical and transverse components (Fig. 5a and 5b). The correlation coefficients of PGV and triggered LFE amplitude of the vertical and transverse components at IGK were 0.90 and 0.74, respectively. The correlation coefficients of PGV and triggered LFE amplitudes of vertical and transverse components at ZMM were 0.89 and 0.78, respectively. The LFEs were triggered at both stations for both components when the PGV was over 0.1 cm/s.

4. Discussion

4.1 Distribution of triggered LFEs and VLFE-LFEs.

The locations of both the triggered LFEs and VLFE-LFEs were close. The triggered LFEs occurred at 24.0°N and 123.6°E in the Yaeyama area and 25.8°N and 127.7°E in the Okinawa area (Fig. 4), very close to those of the VLFE-LFEs, which were determined by using the S-wave arrival time (Nakamura 2017) (Fig. 4). The VLFE-LFEs were distributed at 24.0°N and 123.6–124.1°E in the Yaeyama area (Nakamura 2017) (Fig. 4a), and at 25.8°N and 127.7°E in the Okinawa area, respectively (Nakamura 2017) (Fig. 4b). The locations of the triggered LFEs were up-dip of the SSEs in the Yaeyama area, and these were on the southwest side of the SSEs along the trench in the Okinawa area (Fig. 4). This is consistent with the distribution of the VLFE-LFEs.

The distribution of the triggered LFEs did not exactly match that of the VLFE-LFEs in the Yaeyama area. The clusters of the VLFE-LFEs were distributed at 123.6°E and 124.1°E in the Yaeyama area (Fig. 4a). The epicenters of the triggered LFEs corresponded to the cluster at 123.6°E, while these were rare in the cluster at 124.1°E. Because the seismic stations are distributed along the trench, the accuracy of the epicenter determination for the E–W direction is higher and these clusters can be divided (Nakamura 2017)

(Fig. 4a). Therefore, the triggered LFEs would not have occurred in the cluster at 124.1°E, and each cluster of the VLFE-LFEs in the Yaeyama area showed different sensitivity to induce LFEs. The VLFE-LFE activity was higher near the cluster at 123.6°E (Nakamura 2017), which suggests that the sensitivity of inducing LFEs was higher near 123.6°E.

Similarly, although the clusters of VLFEs-LFEs in the Okinawa area were distributed not only at 25.8°N and 127.7°E, but also to the southeast and east of Okinawa Island (Nakamura 2017), the induced LFEs occurred only at 25.8°N and 127.7°E. High VLFEs-LFEs activity in Okinawa were distributed in 25.8°N and 127.7°E clusters. As in the Yaeyama area, this suggests that the sensitivity for inducing LFEs was higher near 25.8°N and 127.7°E.

These results are consistent with those obtained in another subduction zone. The positional relationship between triggered and ambient tremors in subduction zones can be divided into two types. In the first type, the triggered tremor occurs in the region of ambient tremors such as in Taiwan and Aleusian Islands (Peterson et al. 2011; Chao et al. 2013). In the second type, the triggered tremor occurs on the up-dip side of the region of ambient tremors such as in Cascadia and west Shikoku (Kao and Shan 2004; Miyazawa et al. 2008; Kao et al. 2010; Obara et al. 2010; Chao et al. 2013; Chao and Obara 2016). In the case of the Ryukyu Trench, the accuracy of determining the position in the direction parallel to the trench is high, but the accuracy of determining the component perpendicular to the trench is low. Therefore, it is difficult to rule out that the triggered LFEs occurred on the up-dip side of the region of ambient tremors. In Kyushu, at the northern end of the Ryukyu Trench, triggered tremors occurred near the areas where shallow VLFEs and tremors occurred (Obara and Ito 2005; Yamashita et al. 2015; Chao and Obara 2016). This is consistent with the positional relationship between VLFEs-LFEs and triggered LFEs occurring in the Okinawa area and Yaeyama area. Unlike the Kyushu region, deep tremors or LFEs have not been identified in the Okinawa and Yaeyama areas. This indicates that triggered tremors could be common in or around the shallow VLFE and tremor area along the Ryukyu Trench.

4.2 Threshold for triggered LFEs

The threshold of the PGV, when the LFEs were triggered by Rayleigh and Love waves, was 0.1 cm/s at IGK and ZMM. Here, we converted the PGV to dynamic stress ($\Delta\sigma$). The phase velocity (v) of the Rayleigh and Love waves were set to 4.0 km/s and 3.4 km/s, respectively. Rigidity (G) was set to 35 GPa. The dynamic stress can be expressed as follows (Chao and Obara 2016):

$$\Delta\sigma = G\dot{\varepsilon}/v$$

According to this equation, the PGV of 0.1 cm/s corresponds to 8.7–10 kPa. This suggests that LFEs can be triggered by the dynamic stress in the order of 10 kPa in Okinawa and Yaeyama. In a previous study, a

tremor was detected in the southwestern part of the Ryukyu Arc when the dynamic stress was above 5 kPa (Chao and Obara 2016), which is of the same order of magnitude as our result.

A positive correlation between the PGV of the surface wave and the mean amplitude of the tremor has been previously reported at YNG (Chao and Obara 2016). Our results show that there is a strong positive correlation between the LFE data and surface wave amplitude in both Yaeyama and Okinawa, and the triggering threshold is similar in both areas.

A similar correlation between the mean LFE amplitude and PGV of the surface wave was observed in other parts of the tremor area (Chao et al. 2012a; Chao and Obara 2016), which can be explained with the clock advanced model; the LFE activity is accelerated by the addition of dynamic stress to the fault plane where ambient tremors occur (Gomberg 2010; Chao et al. 2013). This indicates that ambient tremors are activated by stress acceleration in the Yaeyama and Okinawa areas and the LFEs observed in these areas can be the result of the activation of the ambient tremors due to increased stress. While LFEs have been observed in these areas, ambient tremors have not been observed in land-based networks. Since there are no low-noise borehole-type seismometers in this region, only a large amplitude of the ambient tremors can be detected as LFEs. Highly sensitive seismic observations in these areas will enable us to detect the occurrence of ambient tremors.

Here, we discuss the reasons the LFEs were not observed while the PGV was large enough to trigger the LFEs when the 2011 Tohoku-Oki earthquake occurred. The PGVs of the radial and transverse components of the 2011 Tohoku-Oki earthquake (Mw9.0) were 0.53 cm/s and 0.60 cm/s, respectively, at IGK, and 0.60 cm/s and 0.69 cm/s, respectively, at ZMM (Fig. 5a and 5b). These values were over the threshold (0.10 cm/s) to trigger the LFEs. Applying the PGV at ZMM and IGK to the linear relationship between the PGV and triggered LFE amplitudes, the amplitude of the triggered LFE can be estimated as 30 nm/s. However, no LFE was observed in the Okinawa and Yaeyama areas. We assume that the large background noise at the time of the passage of the surface wave of the 2011 earthquake obscured the detection of the triggered LFEs. The median amplitudes at the frequency range of 2–4 Hz at ZMM and IGK were on the order of 100 nm/s during the passage of the surface wave of the 2011 earthquake. It is possible that the coda part of the body wave was not sufficiently small when the surface wave passed because the epicentral distance was not far enough (approximately 2000 km) and the triggered LFEs were obscured by the coda part of the body wave and could not be detected.

The arrival direction of the surface wave of the large PGV earthquakes was skewed southwestward except for the 2011 earthquake. Therefore, it was not possible to evaluate whether the threshold of the triggered LFE was azimuthally dependent or not.

5. Conclusions

We determined the distribution of the triggered LFEs by dynamic stress changes in the surface waves in the central and southern areas of the Ryukyu Trench. The LFEs triggered by the surface waves of a large earthquake in the Ryukyu Islands were distributed to the south of the Okinawa and Yaeyama areas.

These locations were overall consistent with the clusters of VLFEs-LFEs in this area. The triggered LFE activity was limited to the clusters in which the VLFEs-LFEs were originally active. This suggests that each cluster of the VLFEs-LFEs in the Yaeyama area had a different sensitivity to trigger LFEs.

The epicenters of the triggered LFEs in the Okinawa and Yaeyama areas are in or near the shallow VLFE area. This is consistent with the relationship between triggered tremors and shallow VLFEs observed in the Kyushu region at the northern end of the Ryukyu Trench. This indicates that triggered tremors could be common in or around the shallow VLFE and tremor area along the Ryukyu Trench.

The LFEs were triggered when the PGV of the surface waves was higher than 0.1 cm/s, and the mean amplitudes of LFEs showed a positive correlation with the PGV of the surface waves. This condition is similar to that in other areas where triggered tremors have been observed, which suggests that the LFEs observed in the Ryukyu Trench can be the result of the activation of ambient tremors due to increased stress.

Abbreviations

JMA: Japan Meteorological Agency

LFE: Low-frequency earthquake

NIED: National Research Institute for Earth Science and Disaster Resilience

OBS: Ocean bottom seismometer

PGV: peak ground velocity

RMS: root-mean-square

SSE: slow slip event

VLFE: very low-frequency earthquake

VLFE-LFE: low-frequency earthquakes accompanied with very-low frequency earthquakes

Declarations

Ethics approval and consent to participate

Not applicable.

Consent for publication

Not applicable.

Availability of data and materials

The datasets used in this study are available from AK and MN upon reasonable request.

Competing interests

The authors declare that they have no competing interests.

Funding

This research was supported by JSPS KAKENHI Grant Number JP16H06473 for a Scientific Research on Innovative Areas program titled “Science of Slow Earthquakes”; funding was also provided by the Tokyo Marine Kagaki Memorial Foundation.

Authors’ Contributions

AK carried out the analyses and wrote the manuscript. NM contributed to the interpretations and presentation of the manuscript. All authors read and approved the final manuscript.

References

1. Arai R, Takahashi T, Kodaira S, Kaiho Y, Nakanishi A, Fujie G, Nakamura Y, Yamamoto Y, Ishihara Y, Miura S, Kaneda Y (2016) Structure of the tsunamigenic plate boundary and low-frequency earthquakes in the southern Ryukyu Trench. Nat Commun 7:12255. https://doi.org/10.1038/ncomms12255
2. Chao K, Peng Z, Fabian A, Ojha L (2012a) Comparisons of triggered tremor in California. Bull Seismol Soc Am 102(2):900–908. https://doi.org/10.1785/0120110151
3. Chao K, Peng Z, Wu C, Tang CC, Lin CH (2012b) Remote triggering of non-volcanic tremor around Taiwan. Geophys J Int 188:301–324. https://doi.org/10.1111/j.1365-246X.2011.05261.x
4. Chao K, Peng Z, Gonzalez-Huizar H, Aiken C, Enescu B, Kao H, Velasco AA, Obara K, Matsuzawa T (2013) A Global Search for Triggered Tremor Following the 2011 Mw 9.0 Tohoku Earthquake. Bull Seism Soc Am 103:1551–1571. https://doi.org/10.1785/0120120171
5. Chao K, Obara K (2016) Triggered tectonic tremor in various types of fault systems of Japan following the 2012 Mw8.6 Sumatra earthquake. J Geophys Res 121:170–187. https://doi.org/10.1002/2015JB012566
6. Fry B, Chao K, Bannister S, Peng Z (2011) Deep tremor beneath the Hikurangi margin in New Zealand triggered by the 2010 Mw 8.8 Chile earthquake. Geophys Res Lett 38:L15306. doi:10.1029/2011GL048319

7. Gomberg J, Rubinstein JL, Peng Z (2008) Widespread triggering of nonvolcanic tremor in California. Science 319:173. http://doi.org/10.1126/science.1149164
8. Gomberg J (2010) Lessons from (triggered) tremor. J Geophys Res 115:B10302. doi:10.1029/2009JB007011
9. Hayers GP, Wald DJ, Johnson RL (2012) Slab1.0: A three-dimensional model of global subduction zone geometries. J Geophys Res 117:B01303. https://doi.org/10.1029/2011JB008524
10. Ide S (2012) Variety and spatial heterogeneity of tectonic tremor worldwide. J Geophys Res 117:B03302. https://doi.org/10.1029/2011JB008840
11. Ito Y, Hino R, Suzuki S, Kaneda Y (2015) Episodic tremor and slip near the Japan Trench prior to the 2011 Tohoku-Oki earthquake. Geophys Res Lett 42:1725–1731. https://doi.org/10.1002/2014GL062986
12. Kao H, Shan SJ (2004) The Source-Scanning Algorithm: Mapping the distribution of seismic sources in time and space. Geophys J Int 157(2):589–594. https://doi.org/10.1111/j.1365-246X.2004.02276.x
13. Kao H, Wang K, Dragert H, Kao JY, Rogers G (2010) Estimating seismic moment magnitude (Mw) of tremor bursts in northern Cascadia: Implications for the “seismic efficiency” of episodic tremor and slip. Geophys Res Lett 37(19):L19306. https://doi.org/10.1029/2010GL044927
14. Miyazawa M, Mori J (2006) Evidence suggesting fluid flow beneath Japan due to periodic seismic triggering from the 2004 Sumatra-Andaman earthquake. Geophys Res Lett 33:L05303. https://doi.org/10.1029/2005GL025087
15. Miyazawa M, Brodsky E, Mori J (2008) Learning from dynamic triggering of low-frequency tremor in subduction zones. Earth Planets Space 60:e17–e20. https://doi.org/10.1186/BF03352858
16. Nadeau R, Dolenc D (2005) Nonvolcanic tremors deep beneath the San Andreas fault. Science 307(5708):389. https://doi.org/10.1126/science.1107142
17. Nakamura M (2017) Distribution of low-frequency earthquakes accompanying the very low frequency earthquakes along the Ryukyu Trench. Earth Planets Space 69:49. http://doi.org/10.1186/s40623-017-0632-4
18. Nishimura T (2014) Short-term slow slip events along the Ryukyu Trench, southwestern Japan, observed by continuous GNSS. Prog Earth Planet Sci 1:22. http://doi.org10.1186/s40645-014-0022-5
19. Obara K (2002) Nonvolcanic deep tremor associated with subduction in southwest Japan. Science 296:1679–1681. https://doi.org/10.1126/science.1070378
20. Obara K, Ito Y (2005) Very low frequency earthquakes excited by the 2004 off the Kii peninsula earthquakes—A dynamic deformation process in the large accretionary prism. Earth Planets Space 57(4):321–326. https://doi.org/10.1186/BF03352570
21. Obara K, Kodaira S (2009) Low-frequency tremors associated with reverse faults in a shallow accretionary prism. Earth Planet Sci Lett 287:168–174. https://doi.org/10.1016/j.epsl.2009.08.005

22. Obara K, Tanaka S, Maeda T, Matsuzawa T (2010) Depth-dependent activity of non-volcanic tremor in southwest Japan. Geophys Res Lett 37(13):L13306. http://doi.org/10.1029/2010GL043679
23. Obara, K, Ito Y (2005) Very low frequency earthquakes excited by the 2004 off the Kii peninsula earthquakes—A dynamic deformation process in the large accretionary prism. Earth Planets Space, 57(4), 321–326. https://doi.org/10.1186/BF03352570
24. Obara K, Kato A (2016) Connecting slow earthquakes to huge earthquakes. Science 353:253–257. https://doi.org/10.1126/science.aaf1512
25. Payero J, Kostoglodov V, Shapiro N, Mikumo T, Iglesias A, Pérez-Campos X, Clayton R (2008) Nonvolcanic tremor observed in the Mexican subduction zone. Geophys Res Lett 35(7):L07305. https://doi.org/10.1029/2007GL032877
26. Peng Z, Vidale JE, Creager KC, Rubinstein JL, Gomberg J, Bodin P (2008) Strong tremor near Parkfield, CA, excited by the 2002 Denali Fault earthquake. Geophys Res Lett 35:L23305. https://doi.org/10.1029/2008GL036080
27. Peterson C, McNutt S, Christensen D (2011) Nonvolcanic tremor in the Aleutian Arc. Bull Seismol Soc Am 101(6):3081–3087. https://doi.org/10.1785/0120100241
28. Rogers G, Dragert H (2003) Episodic tremor and slip on the Cascadia subduction zone: the chatter of silent slip. Science 300(5627):1942–1943. https://doi.org/10.1126/science.1084783
29. Rubinstein JL, Vidale JE, Gomberg J, Bodin P, Creager KC, Malone SD (2007) Non-volcanic tremor driven by large transient shear stresses. Nature 448:579–582. https://doi.org/10.1038/nature06017
30. Sun WF, Peng Z, Lin CH, Chao K (2015) Detecting deep tectonic tremor in Taiwan with a dense array. Bull Seismol Soc Am 105(3):1349–1358. https://doi.org/10.1785/0120140258
31. Tanaka S, Matsuzawa T, Asano Y (2019) Shallow low-frequency tremor in the northern Japan Trench subduction zone. Geophys Res Lett 46:5217–5224. https://doi.org/10.1029/ 2019GL082817
32. Ueno H, Hatakeyama S, Aketagawa T, Funasaki J, Hamada N (2002) Improvement of hypocenter determination procedures in the Japan Meteorological Agency (in Japanese). Quart J Seis 65:123–134.
33. Walter JI, Schwartz SY, Protti JM, Gonzalez V (2011) Persistent tremor within the northern Costa Rica seismogenic zone. Geophys Res Lett 38:L01307. https://doi.org/10.1029/2010GL045586
34. Wessel P, Smith W (1998) New, improved version of Generic Mapping Tools released. Eos Trans AGU 79 (47):579. https://doi.org/10.1029/98EO00426
35. Yamashita Y, Yakiwara H, Asano Y, Shimizu H, Uchida K, Hirano S, Umakoshi K, Miyamachi H, Nakamoto M, Fukui M, Kamizono M, Kanehara H, Yamada T, Shinohara M, Obara K (2015) Migrating tremor off southern Kyushu as evidence for slow slip of a shallow subduction interface. Science 348(6235):676–679. https://doi.org/10.1126/science.aaa4242

Figures

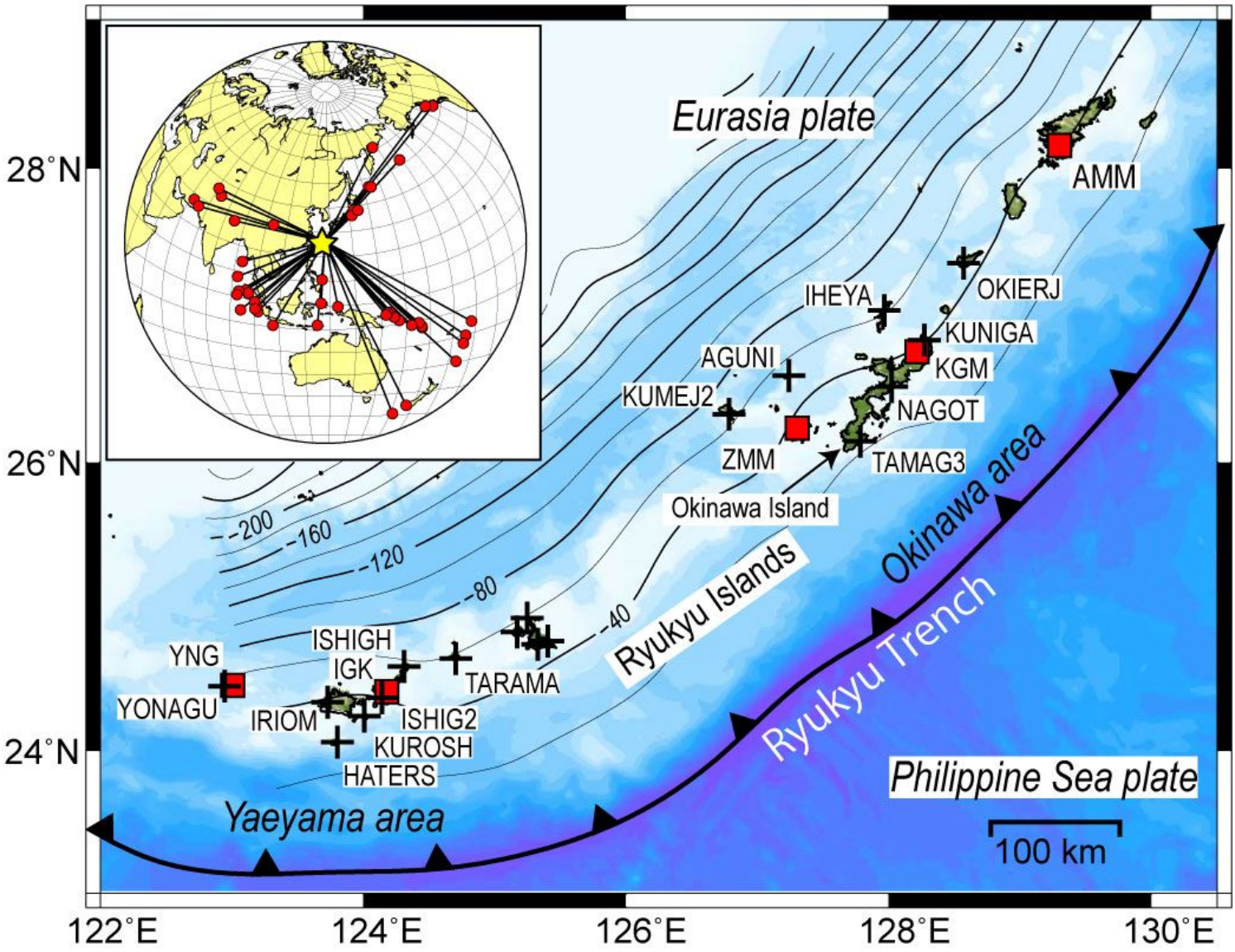

Figure 1

Distribution of the seismic stations. Squares denote the Fnet stations, and the crosses denote the JMA stations. Solid black contours show the depth of the plate interface (Hayers et al. 2012). The inset shows the distribution of the teleseismic earthquakes (red circles) used in this study. Note: The designations employed and the presentation of the material on this map do not imply the expression of any opinion whatsoever on the part of Research Square concerning the legal status of any country, territory, city or area or of its authorities, or concerning the delimitation of its frontiers or boundaries. This map has been provided by the authors.

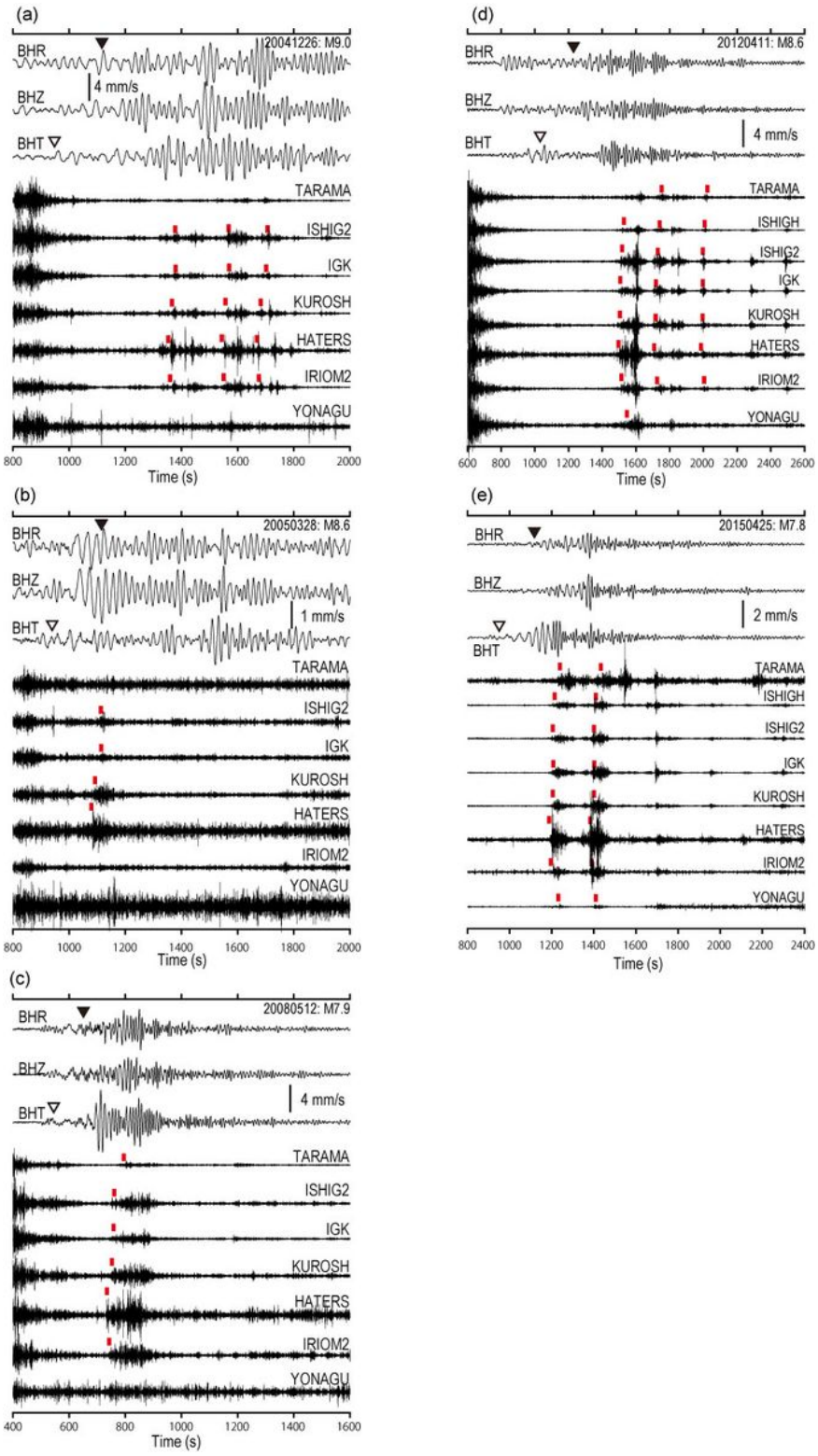

Figure 2

Waveforms of the triggered LFEs observed in the Yaeyama area. (a) Broadband and short-period seismographs of the 2004 Sumatra earthquake. Upper part shows the instrumentally corrected broadband seismograph at IGK. Zero time denotes the occurrence time of the earthquake. The black and white triangles denote the estimated arrival time of the Rayleigh and Love waves, respectively. The velocity of the Rayleigh and Love waves is assumed to be 4.0 km/s and 3.4 km/s, respectively. The thick

vertical bar shows the scale of the broadband seismograph. Lower part shows the 2–4 Hz band-pass filtered short-period seismograph of the N–S component. The triggered LFEs were recorded at several stations. The waveforms are plotted from western stations to eastern stations along the trench. (b) Same as (a) but for the 2005 Nias earthquake. (c) Same as (a) but for the 2008 Wenchuan earthquake. (d) Same as (a) but for the 2012 Sumatra earthquake. (e) Same as (a) but for the 2015 Nepal earthquake.

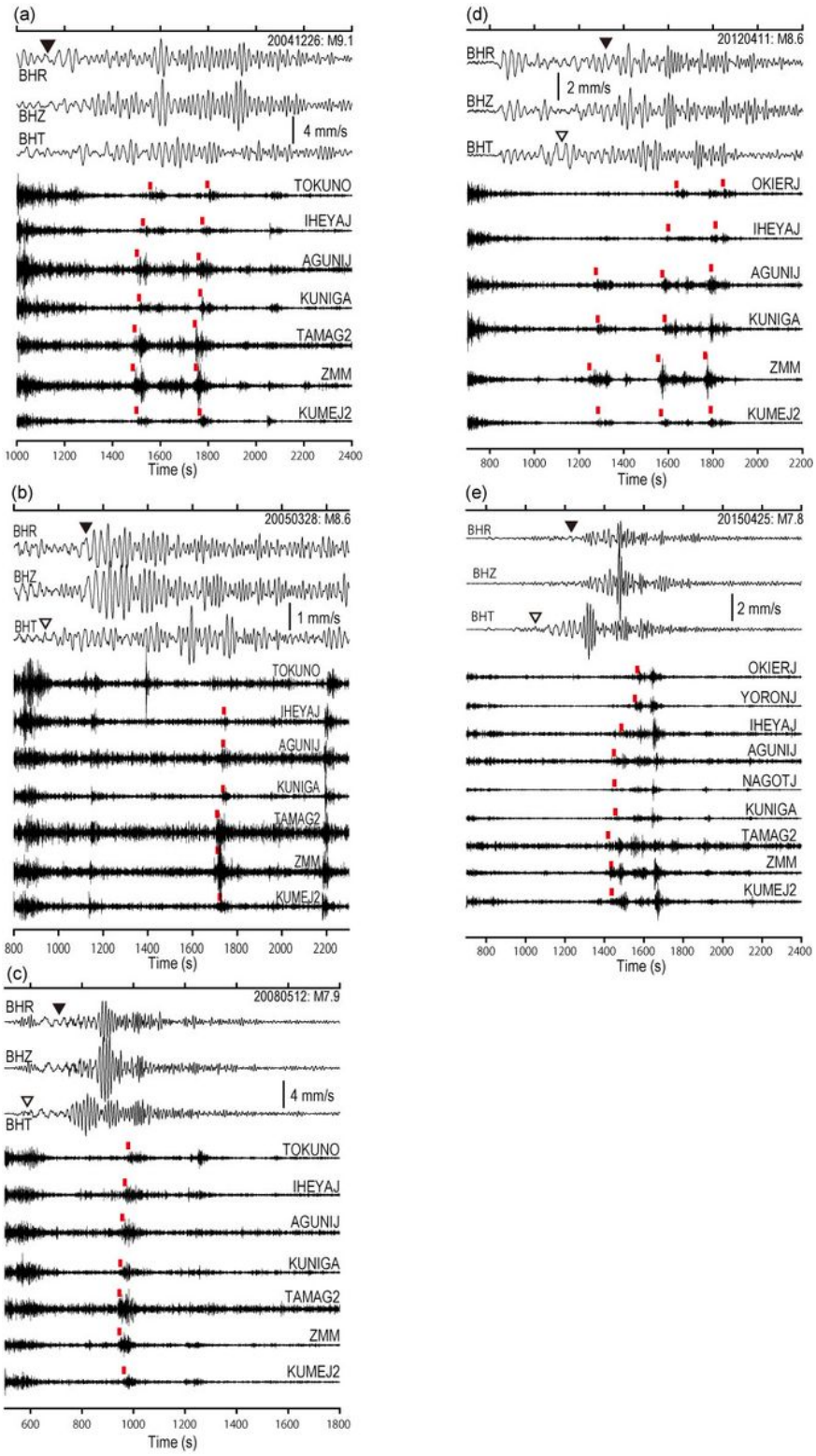

Figure 3

Waveforms of the triggered LFEs observed in the Okinawa area. (a) Broadband and short-period seismographs of the 2004 Sumatra earthquake. Upper part shows the instrumentally corrected broadband seismograph at ZMM. Zero time denotes the occurrence time of the earthquake. The black and white triangles denote the estimated arrival time of the Rayleigh and Love waves, respectively. The velocity of the Rayleigh and Love waves is assumed to be 4.0 km/s and 3.4 km/s, respectively. The thick vertical bar shows the scale of the broadband seismograph. Lower part shows the 2–4 Hz band-pass filtered short-period seismograph of the N–S component. The triggered LFEs were recorded at several stations. The waveforms are plotted from southwestern stations to northeastern stations along the trench. (b) Same as (a) but for the 2005 Nias earthquake. (c) Same as (a) but for the 2008 Wenchuan earthquake. (d) Same as (a) but for the 2012 Sumatra earthquake. (e) Same as (a) but for the 2015 Gorkha earthquake.

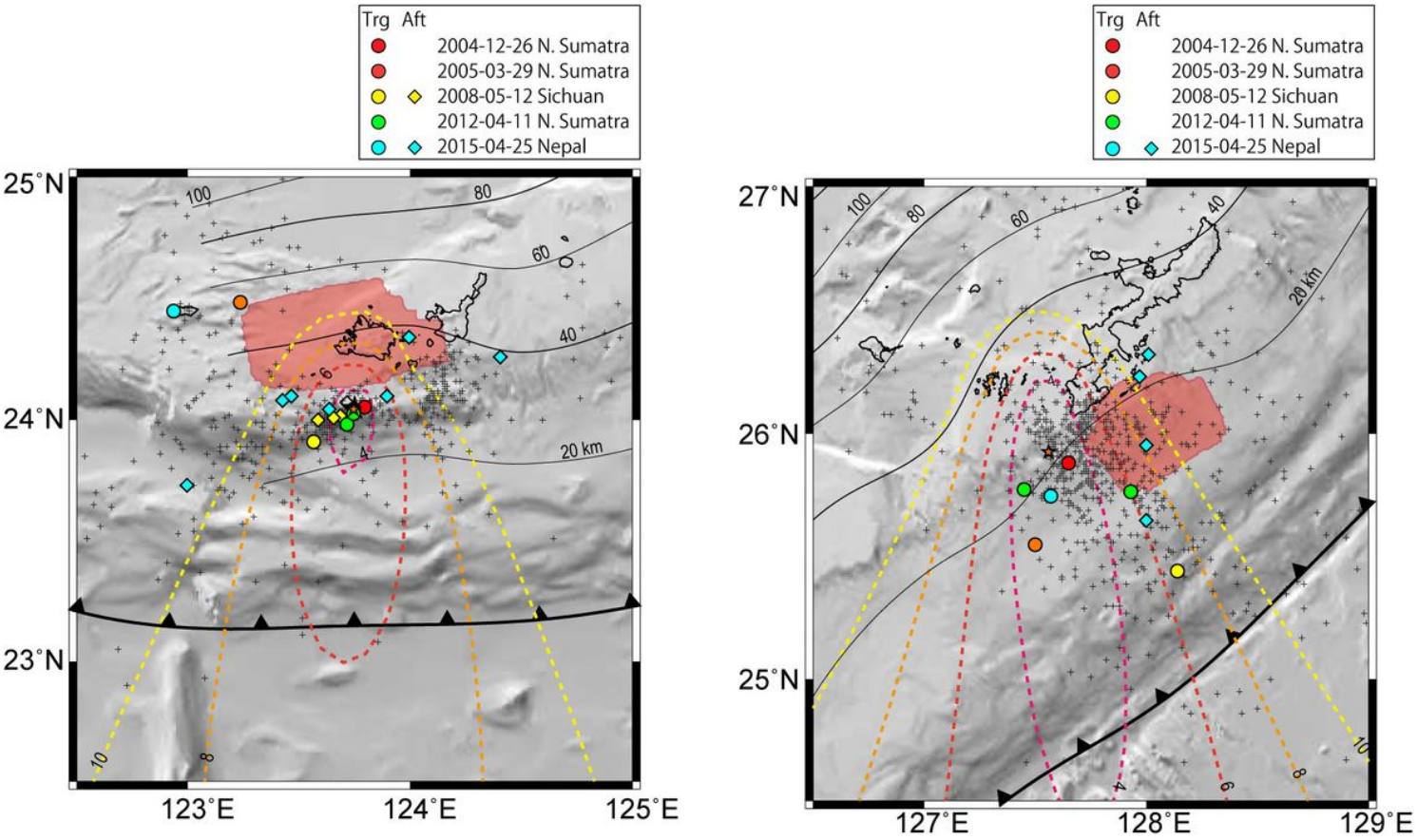

Figure 4

Epicentral distribution of the LFEs. (Left) Epicentral distribution of the LFEs in the Yaeyama area. Circles show the epicenter of the triggered LFEs during the passage of the surface waves. Diamonds denote the epicenters of LFEs after the passage of the surface waves. Colors of the circles and diamonds are different for each teleseismic event. The crosses show the epicenters of VLFE-LFEs (Nakamura 2017). The red hatch shows the slow slip event (SSE) area where the number of SSEs was over 5 (Nishimura 2014). The dotted contours show the RMS errors of the LFEs (denoted by stars) accompanying the surface wave of the 2004 Sumatra earthquake. The black colored contour shows the depth of the plate interface (Hayer et al. 2012). (Right) Same as (a) but for the Okinawa area.

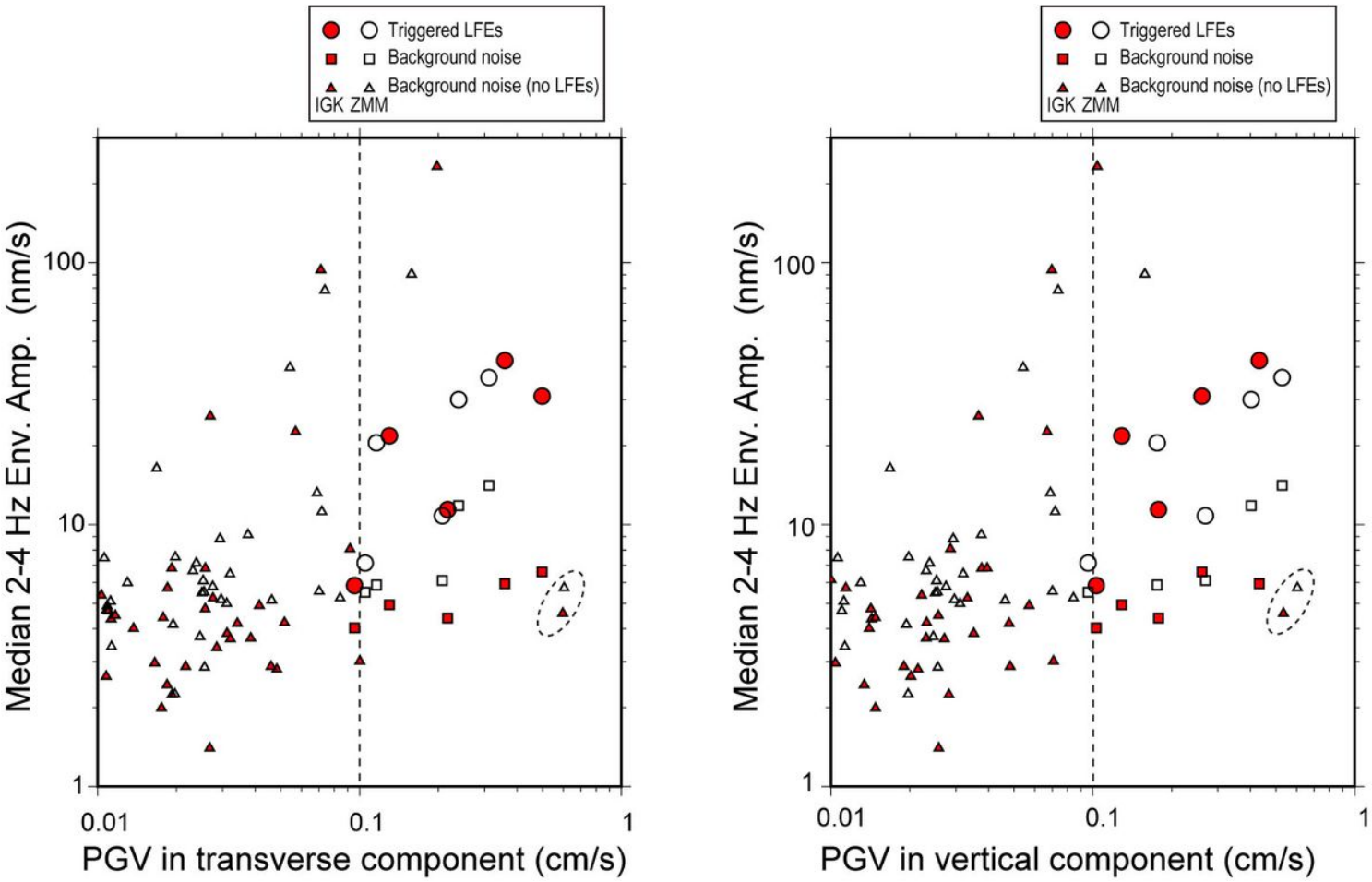

Figure 5

Median 2–4 Hz envelope amplitude of triggered LFEs and background noise as a function of (a) PGV in transverse components and (b) PGV in vertical components at IGK and ZMM. Background noise level of each event was computed at 0–300 s before the occurrence of the mainshock. Circles, squares, and triangles show the data points for triggered LFEs, background noise level, and background noise level of the event where the triggered LFEs were not observed, respectively. Solid and open marks show the data points at IGK and ZMM, respectively. Ellipses show the data for the 2011 Tohoku-Oki earthquake.

Supplementary Files

This is a list of supplementary files associated with this preprint. Click to download.

- GraphycalAbst.jpg
- TableS120210226.xlsx
- TableS220210226.xlsx